A heterogeneous lunar interior for hydrogen isotopes as revealed by the lunar highlands samples

Hejiu Hui [a,b,*], Yunbin Guan [c], Yang Chen [d], Anne H. Peslier [e], Youxue Zhang [f], Yang Liu [d], Roberta L. Flemming [g], George R. Rossman [c], John M. Eiler [c], Clive R. Neal [b], Gordon R. Osinski [g]

[a] *State Key Laboratory for Mineral Deposits Research & Lunar and Planetary Science Institute, School of Earth Sciences and Engineering, Nanjing University, Nanjing, Jiangsu 210023, China*
[b] *Department of Civil and Environmental Engineering and Earth Sciences, University of Notre Dame, Notre Dame, IN 46556, USA*
[c] *Division of Geological and Planetary Sciences, California Institute of Technology, Pasadena, CA 91125, USA*
[d] *Jet Propulsion Laboratory, California Institute of Technology, Pasadena, CA 91109, USA*
[e] *Jacobs, NASA-Johnson Space Center, Mail Code XI3, Houston, TX 77058, USA*
[f] *Department of Earth and Environmental Sciences, University of Michigan, Ann Arbor, MI 48109, USA*
[g] *Department of Earth Sciences & Centre for Planetary Science and Exploration, University of Western Ontario, London, Ontario N6A 5B7, Canada*

A R T I C L E   I N F O

A B S T R A C T

Knowing the amount and timing of water incorporation into the Moon has fundamental implications for our understanding of how the Earth–Moon system formed. Water has been detected in lunar samples but its abundance, distribution and origin are debated. To address these issues, we report water concentrations and hydrogen isotope ratios obtained by secondary ion mass spectrometry (SIMS) of plagioclase from ferroan anorthosites (FANs), the only available lithology thought to have crystallized directly from the lunar magma ocean (LMO). The measured water contents are consistent with previous results by Fourier transform infrared spectroscopy (FTIR). Combined with literature data, δD values of lunar igneous materials least-degassed at the time of their crystallization range from -280 to $+310‰$, the latter value being that of FAN 60015 corrected for cosmic ray exposure. We interpret these results as hydrogen isotopes being fractionated during degassing of molecular hydrogen (H_2) in the LMO, starting with the magmatic δD value of primordial water at the beginning of LMO being about $-280‰$, evolving to about $+310‰$ at the time of anorthite crystallization, i.e. during the formation of the primary lunar crust. The degassing of hydrogen in the LMO is consistent with those of other volatile elements. The wide range of δD values observed in lunar igneous rocks could be due to either various degrees of mixing of the different mantle end members, or from a range of mantle sources that were degassed to different degrees during magma evolution. Degassing of the LMO is a viable mechanism that resulted in a heterogeneous lunar interior for hydrogen isotopes.

© 2017 Elsevier B.V. All rights reserved.

1. Introduction

The detection of indigenous water in lunar pyroclastic glass beads (Saal et al., 2008) and olivine melt inclusions (Hauri et al., 2011; Chen et al., 2015) has challenged the view held during the Apollo era that the Moon must be "dry" (Taylor et al., 2006). Since the breakthrough discovery of Saal et al. (2008), the abundance, origin and evolution of water in the lunar interior have puzzled

scientists, with scarce data and controversial interpretations. It is still debated how the lunar mantle acquired its volatiles (e.g., Barnes et al., 2016) and also how much water is actually present in the lunar interior (e.g., Boyce et al., 2014). The water contents of melt inclusions in the olivine of pyroclastic sample 74220 have been used to infer that the lunar mantle could have contained an amount of water similar to that of the terrestrial upper mantle (Hauri et al., 2011; Chen et al., 2015). The water detected in plagioclase from ferroan anorthosite (FAN) using Fourier transform infrared spectroscopy (FTIR; Hui et al., 2013) implies that water was present in an early Moon at the time of plagioclase crystallization in the LMO. However, there are uncertainties with calculations of how much might have been retained in the early stage of the

LMO, especially as degassing was not considered in this study (Hui et al., 2013). A recent study (Mills et al., 2017) found ∼20 ppm (by weight as H_2O, and hereafter) in alkali feldspar from potassium-enriched rocks, implying magmatic water contents of ∼1 wt% in chemically evolved rhyolitic magmas. In contrast, Cl, Zn and K isotopes, and Zn concentrations in lunar rocks are more compatible with a volatile-depleted lunar interior (Sharp et al., 2010; Paniello et al., 2012; Albarède et al., 2015; Kato et al., 2015; Wang and Jacobsen, 2016). Finally, although some lunar apatites contain water (Greenwood et al., 2011; Barnes et al., 2014; Tartèse et al., 2014), this does not necessarily provide significant constraints on the water content of the magma that the apatite crystallized from (Boyce et al., 2014).

The interpretation of hydrogen isotope ratios of lunar materials is even more complicated. Hydrogen has two stable isotopes, H and D, and their relative abundance is expressed as δD, i.e. $\delta D = ((D/H)_{sample}/(D/H)_{standard} - 1) \times 1000$, where the standard is VSMOW. Greenwood et al. (2011) proposed that the water comes from the lunar mantle, solar wind protons, and/or comets evidenced by the large variation of hydrogen isotopic ratios ($\delta D = -202$ to $+1010‰$) in lunar apatite from mare basalts and highland rocks. Furthermore, the very low δD ($<-550‰$) of most lunar agglutinates indicate that solar wind protons are a major source of the hydrogen in lunar regolith (Liu et al., 2012). Stephant and Robert (2014) agreed that hydrogen in the lunar regolith is mostly from solar wind implantation, but argued that the D/H ratio can be increased during cosmic ray spallation. Treiman et al. (2016) suggested that the lowest δD of lunar basalts ($\delta D \leq -100‰$) could have resulted from assimilation of solar-wind-implanted lunar regolith, while their high δD (up to ∼$+1100‰$) most reasonably indicates that indigenous magmatic hydrogen partially degassed molecular hydrogen (H_2). Füri et al. (2014) reported δD of $+38‰$ to $+809‰$ in lunar 74002 volcanic glasses and inferred an initial δD of the order of $-100‰$ and a water content of 100–300 ppm H_2O for the primary magma.

Among lithologies analyzed for water content and hydrogen isotopes (e.g., Boyce et al., 2010; McCubbin et al., 2010; Saal et al., 2013; Tartèse et al., 2013; Anand et al., 2014; Robinson and Taylor, 2014; Barnes et al., 2016; Robinson et al., 2016; Mills et al., 2017), plutonic rocks and olivine-hosted melt inclusions are likely the least affected by degassing of hydrogen-bearing species and assimilation of regolith. Therefore, these least modified hydrogen isotope ratios may best represent those in the lunar interior. Two contrasting observations have been obtained: low hydrogen isotope ratios of highland noritic apatites ($\delta D = -281$ to $-27‰$; Barnes et al., 2014) and of some "undegassed" KREEP (K + REE [rare earth elements] + P) apatites ($\delta D = -130 \pm 50‰$; Tartèse et al., 2014); and high hydrogen isotope ratios and pre-eruptive water content of the least degassed olivine-hosted melt inclusion measured ($\delta D = +187‰$, 1144 ppm H_2O; Saal et al., 2013) from pyroclastic sample 74220. Saal et al. (2013) interpreted the high δD of olivine-hosted melt inclusions as representing an upper limit on the primary value of the magma in the lunar interior. The large range of δD in primitive lunar igneous rocks is so far poorly understood and the origin and evolution of water of the Moon's interior is still unconstrained.

One major complication regarding the sources of lunar water is that geologic processes (e.g., late addition and magmatic degassing) may have modified the hydrogen isotopic ratios of lunar materials. It has been proposed that some water may have been added to the lunar mantle and regolith by later impacts (Elkins-Tanton and Grove, 2011; Greenwood et al., 2011). Conversely, a decrease of water content and an increase of D/H ratio in crystallizing magma could have resulted from degassing of H_2 (Saal et al., 2013; Füri et al., 2014; Tartèse et al., 2014). Therefore, given the limited amount of data and possible late-stage pro-

cesses, it may be difficult (if not impossible) to assess the effects on hydrogen of the magmatic processes that could have occurred in the Moon and to infer the initial hydrogen concentration of the LMO. Previous hydrogen isotope studies (e.g., Greenwood et al., 2011; Liu et al., 2012; Saal et al., 2013; Barnes et al., 2014; Füri et al., 2014; Tartèse et al., 2014; Stephant and Robert, 2014; Treiman et al., 2016) were all targeting samples derived from partial melting of the lunar mantle. The latter crystallized from the LMO, thus these samples have the potential to sample hydrogen signatures from events occurring after LMO crystallization. Furthermore, lunar basalts erupted in a vacuum and have undergone extensive degassing, which fractionates hydrogen isotopes (Saal et al., 2013). In contrast, water detected in plagioclases from FAN samples, which presumably crystallized directly from the LMO, allowed us to speculate that the LMO could have contained ∼320 ppm H_2O (Hui et al., 2013). Note that this concentration should be revised to ∼136 ppm, taking into account new FTIR absorption coefficient for plagioclase (Mosenfelder et al., 2015) and new partition coefficient for hydrogen between plagioclase and melt (Hamada et al., 2013). The fact that water is detectable in these FANs presents the best opportunity for determining δD of the only available lunar lithology directly formed from the LMO (e.g., Shearer et al., 2006). This assumes that shock has minimal effects on hydrogen content and isotopic ratios of plagioclase, which will be discussed because ferroan anorthosites have experienced various degrees of impact on the Moon's surface. Here, we present hydrogen isotope measurements in lunar FAN lithologies and address the origin of water in the early Moon.

2. Samples studied

Lunar plagioclase grains selected for this study are from ferroan anorthosites 15415,238 and 60015,787, and Mg-suite troctolite 76535,164 and are the same grains previously analyzed for water contents using FTIR (Hui et al., 2013). A summary of the samples' characteristics (Hui et al., 2013) is presented here.

Sample 15415, which was collected on the rim of Apur Crater during the Apollo 15 mission, is a chemically pristine coarse-grained ferroan anorthosite made up of >98% anorthite ($An_{96.6–98.2}$) and accessory pyroxene (Morgan et al., 1972; Dixon and Papike, 1975; McGee, 1993). Ferroan anorthosite 60015 is covered by a rind of thick black glass and was collected near the Lunar Module during the Apollo 16 mission (Dixon and Papike, 1975). No crystallization ages using isochron dating methods have been determined for these two ferroan anorthosites, but it is generally believed that ferroan anorthosite are relics of primary feldspathic lunar crust having formed by accumulating plagioclase crystallizing from the LMO by floatation (Norman et al., 2003; Shearer et al., 2006). However, this simple LMO model may not explain the whole range of Mg# (Mg# = molar $Mg/(Mg + Fe^{2+})$) in mafic minerals exhibited by anorthosites from lunar feldspathic meteorites (Gross et al., 2014). An age of 4.46 ± 0.04 Ga has been determined for the crystallization age of lunar ferroan anorthosites using an ^{147}Sm–^{143}Nd isochron based on mafic fractions from four different ferroan anorthosites (60025, 62236, 67016c, and 67215c; Norman et al., 2003). However, younger ages have also been reported for some ferroan anorthosites (Borg et al., 2011, 2015). This suggests that the LMO may have cooled over an extended duration (Elkins-Tanton et al., 2011; Borg et al., 2015) or that these samples are comprised of clasts of different ages, not all primary products of the LMO.

Sample 76535, collected at Station 6 during the Apollo 17 mission, is an Mg-suite troctolite. This coarse-grained plutonic rock is composed of 60% olivine ($Fo_{87.3}$), 35% plagioclase ($An_{96.2}$) and 5% orthopyroxene ($En_{84.1}Wo_{0.9}$) (Dymek et al., 1975). It has been shown that troctolite 76535 is chemically pristine
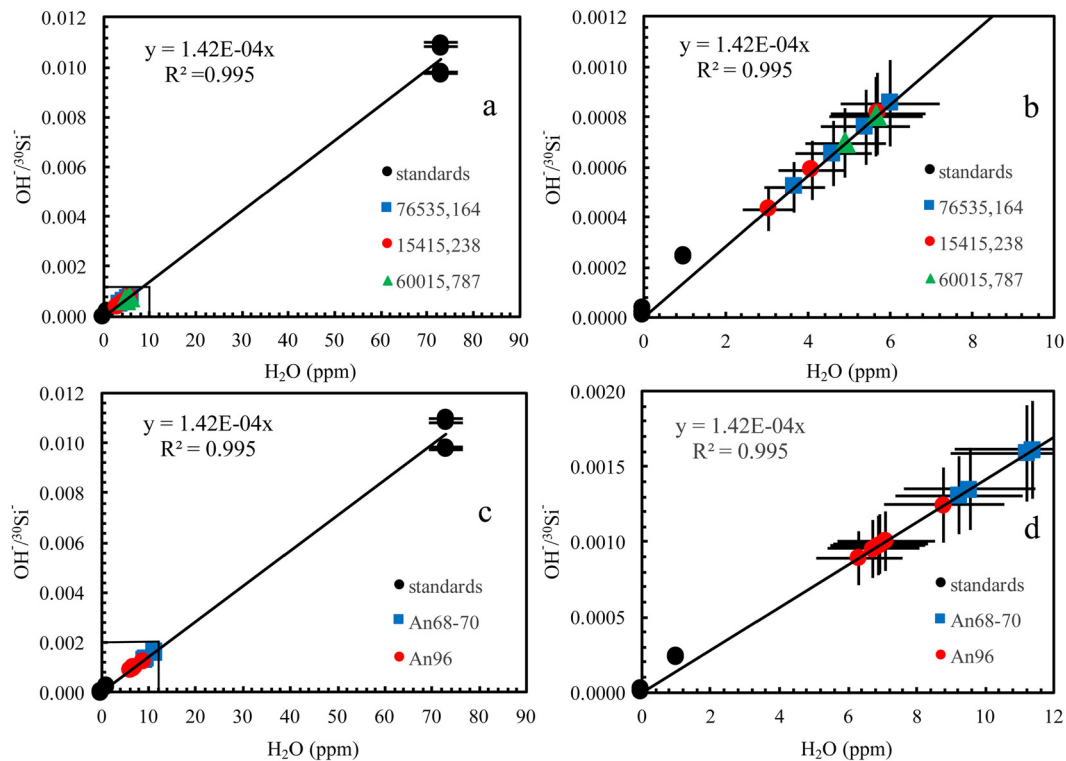
Fig. 1. Calibration curves for SIMS determination of H_2O contents in lunar highland (a), (b) and terrestrial plagioclases (c), (d) expressed in terms of $OH^-/^{30}Si^-$ ratios. The standards used are dehydrated plagioclase grains (0 ppm), GRR2058 (1 ppm), and GRR1968 (73 ppm, Mosenfelder et al., 2015).

(Day et al., 2010). Borg et al. (2015) determined a crystallization age of 4.306 ± 0.010 Ga using multiple isotopic systematics. The Mg-Suite samples may have resulted from the interaction between the hot early LMO cumulates and the base of the lunar primordial crust during cumulate pile overturn (Shearer et al., 2015). This scenario also indicates a genetic correlation between ferroan anorthosites and the Mg-Suite. These deep-seated plutonic rocks were brought to the lunar surface, possibly by impacts, though it is not clear yet how deep these samples crystallized and when they were excavated.

3. Analytical methods

3.1. Secondary ion mass spectrometry (SIMS)

One piece from a polished plagioclase grain of each sample along with terrestrial plagioclase standards were embedded in an indium disc for SIMS analyses following the protocols of previous studies (Hauri et al., 2002).

Before SIMS analysis, the samples were cleaned and stored in a vacuum oven for about a week. Then, the plagioclase grains were coated with Au–Pd and analyzed with a Cameca ims-7f GEO ion probe at the California Institute of Technology. We generally followed the previous analytical procedure (Hauri et al., 2002; Mosenfelder et al., 2011), with efforts on reducing the hydrogen background during analyses. To minimize hydrogen (and OH) backgrounds, the instrument was baked for 24 h and samples were kept in the sample storage chamber ($\sim 4 \times 10^{-9}$ torr) for about a week prior to analysis. The vacuum for the sample chamber during analysis was $\sim 2 \times 10^{-10}$ torr.

To assess potential hydrogen contamination from sample preparation and minimize the hydrogen background effect of the SIMS, we prepared two sets of plagioclase standards. One set includes four natural gem-quality plagioclase grains with GRR2058 (1 ppm H_2O), and GRR1968 (73 ppm H_2O, Mosenfelder et al., 2015). The

other set consists of three dehydrated plagioclase grains (one piece each from An_{68-70} [from an online vender without source information], An_{96} [Waythomas et al., 2010], and GRR2058), which have been degassed by heating to $\sim 1000\,^\circ$C for about two weeks in a high-purity N_2 atmosphere (99.9999% with less than 0.15 ppm of moisture and O_2, 0.10 ppm of total hydrocarbons and $CO + CO_2$) at the University of Michigan. Both natural and dehydrated grains were cleaned with the same procedure as described in Hui et al. (2013), and analyzed using SIMS under the same conditions.

Lunar plagioclase and standards were mounted in the same indium disc. A $+10$ keV Cs^+ primary beam was used to sputter the sample. Secondary ions of -9 keV ($^{12}C^-$, $^{16}OH^-$, $^{18}O^-$, $^{19}F^-$, $^{30}Si^-$, $^{32}S^-$, $^{35}Cl^-$) were collected at a mass resolving power (MRP) of ~ 5500. Calibration curves for H_2O concentration was done using the dehydrated and two natural plagioclases (H_2O: 0 ppm in the dehydrated grains; 1 ppm in GRR2058; 73 ppm in GRR1968) (Fig. 1). The dehydrated plagioclase standards were analyzed to evaluate the background hydrogen contribution periodically, and the average $OH^-/^{30}Si^-$ counts of dehydrated standards (Fig. 2) were subtracted from sample counts.

Hydrogen isotope analysis was performed following H_2O concentration measurement, by collecting H^- and D^- at a lower MRP (~ 1200). The δD of SIMS blanks is $-360 \pm 50\permil$, and that from E-gun alone is $-390 \pm 50\permil$. The D/H blank was checked on the dehydrated An_{96} plagioclase. Calibration for D/H was conducted using plagioclase GRR1968 with an estimated δD of $-42 \pm 39\permil$ (see Supplementary Material for further details).

3.2. Micro-X-ray diffraction (μXRD)

Micro-X-ray diffraction analyses were performed on each lunar plagioclase grains where SIMS measurements were carried out. After Au–Pd coating on the samples was removed by gentle polishing and the samples were cleaned, μXRD analyses were conducted at the University of Western Ontario following the procedure developed for plagioclase by Pickersgill et al. (2015). A Bruker D8
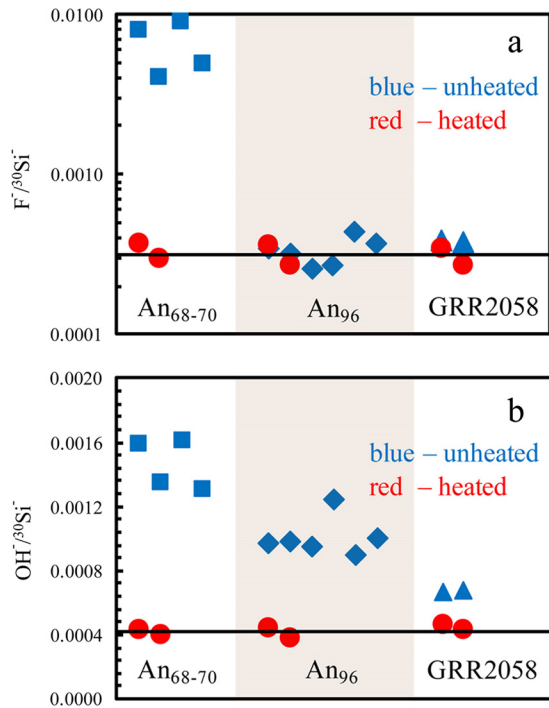
Fig. 2. Comparison of F and OH concentrations in three natural terrestrial plagioclase grains and dehydrated ones.

Table 1

Water contents and hydrogen isotope compositions of lunar (60015, 15415, and 76535) and terrestrial (An$_{68-70}$, An$_{96}$) plagioclase grains analyzed using SIMS in this study.

Sample	C_{H_2O} ppm	C_{H_2O} 2σ ppm	Measured δD ‰	Corrected δD ‰	δD 2σ ‰
60015,787	5	1	430	310	110
15415,238	4	1	1540	280	*500*
76535,164	5	1	1860	−140	*1200*
An$_{68-70}$	10	2	210		50
An$_{96}$	7	1	−10		90

The H$_2$O content of 60015,787 plagioclase by FTIR is 3.4 ppm (Hui et al., 2013) if the new IR absorption coefficient determined for water in plagioclase by Mosenfelder et al. (2015) is used. Corrected δD values are those measured δD after correcting for the contribution of cosmic ray spallation-produced D and H (Saal et al., 2013). The 2σ uncertainties in the δD values are estimated by propagating those in the correction of D and H for the spallation process and in the analytical measurements. Italic font denotes the δD uncertainties are dominated by those in the spallation-produced D and H due to long cosmic ray exposure ages.

Discover diffractometer with theta–theta instrument geometry, a sealed Cobalt source (CoKα radiation) and a 300 μm nominal beam diameter was used, which enabled the sample to remain horizontal and stationary while the source and detector were rotated. For additional information about the technique also see Flemming (2007).

4. Results

4.1. Water contents and hydrogen isotope ratios of lunar plagioclases

SIMS results show that the lunar plagioclase grains of FAN 60015 and 15415, and troctolite 76535 contain 4 to 5 ppm H$_2$O (Fig. 1; Table 1), consistent with FTIR results (Hui et al., 2013; 3.4 ppm H$_2$O for 60015 plagioclase if the new IR absorption coefficient determined for water in plagioclase by Mosenfelder et al. (2015) is used). Furthermore, the water contents contributed from cosmic ray spallation is less than 1 ppm (see below).
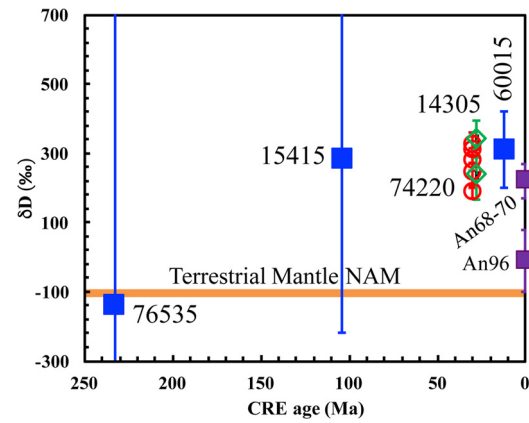

Fig. 3. Hydrogen isotope ratios (δD) of lunar samples [76535 plagioclase (Mg-suite), 15415 and 60015 plagioclase (both FANs), 14305 apatite (highlands alkali-suite; Greenwood et al., 2011), and 74220 olivine-hosted melt inclusion (Saal et al., 2013)] and terrestrial plagioclases [An$_{96}$ and An$_{68-70}$] versus their cosmic ray exposure (CRE) ages. The thick orange line shows the δD range of nominally anhydrous minerals (NAMs) of terrestrial mantle (Bell and Ihinger, 2000). The large uncertainties of 76535 and 15415 plagioclases come mainly from the large corrections for cosmic ray spallation resulting from their prolonged CRE ages. The hydrogen contents of 14305 apatites (Greenwood et al., 2011) and 74220 olivine melt inclusions (Saal et al., 2013) are so high that their corrections for cosmic ray spallation are small enough to be ignored. (For interpretation of the references to color in this figure legend, the reader is referred to the web version of this article.)

The δD values of terrestrial samples An$_{96}$ and An$_{68-70}$ are -10 ± 90‰ and $+210 \pm 50$‰, respectively (Table 1). Sample An$_{68-70}$ has a relatively high δD for a terrestrial plagioclase. However, this grain also contains an extremely high F content, while An$_{96}$, GRR2058 and all heated grains show the same low F counts (i.e., background counts) during SIMS measurements (Fig. 2). Therefore, the high δD and F content are consistent, both indicating a different geological origin from those of the other terrestrial samples.

The measured hydrogen isotope ratios of lunar plagioclase need to be corrected for cosmic ray spallation on the lunar surface (Saal et al., 2013). The cosmic ray exposure (CRE) ages for 76535, 15415, and 60015 are 233 Ma (Lugmair et al., 1976), 104 Ma (Eugster et al., 1984), and 12 Ma (Hörz et al., 1975), respectively. The longer the CRE age, the larger the correction for cosmic ray spallation that needs to be applied, resulting in larger δD uncertainties. After the correction, the δD values for 76535, 15415, and 60015 plagioclases are -140^{+1200}_{-860}‰, $+280 \pm 500$‰, and $+310 \pm 110$‰(2σ), respectively (Fig. 3; Table 1). The large uncertainties, on the δD of 76535 and 15415 render these isotopic ratios meaningless. The corrected δD value ($+310 \pm 110$‰) of FAN 60015 plagioclase, however, is considered reliable due to its relatively young exposure age of ∼12 Ma.

4.2. Shock levels of lunar plagioclases

The shock levels of lunar plagioclases have been assessed using micro-X-ray diffraction. The μXRD images obtained through two-dimensional (2D) general area detector diffraction system (GADDS) show that the plagioclase from the three samples experienced different levels of shock (Fig. 4). The diffraction patterns of our grains from 15415 and 60015 are consistent with previous results obtained by Pickersgill et al. (2015). The shock levels vary from minimally shocked or unshocked for 76535, to moderately shocked for 15415, and to highly shocked for 60015 (Fig. 4). However, none of the grains have become partially or completely isotropic (i.e., maskelynitized or melted) due to impact. This is consistent with the pleochroic bands on FTIR spectra of these grains (Hui et al., 2013), indicating that despite being shocked, the lunar plagioclase grains analyzed here have retained their anisotropic character.
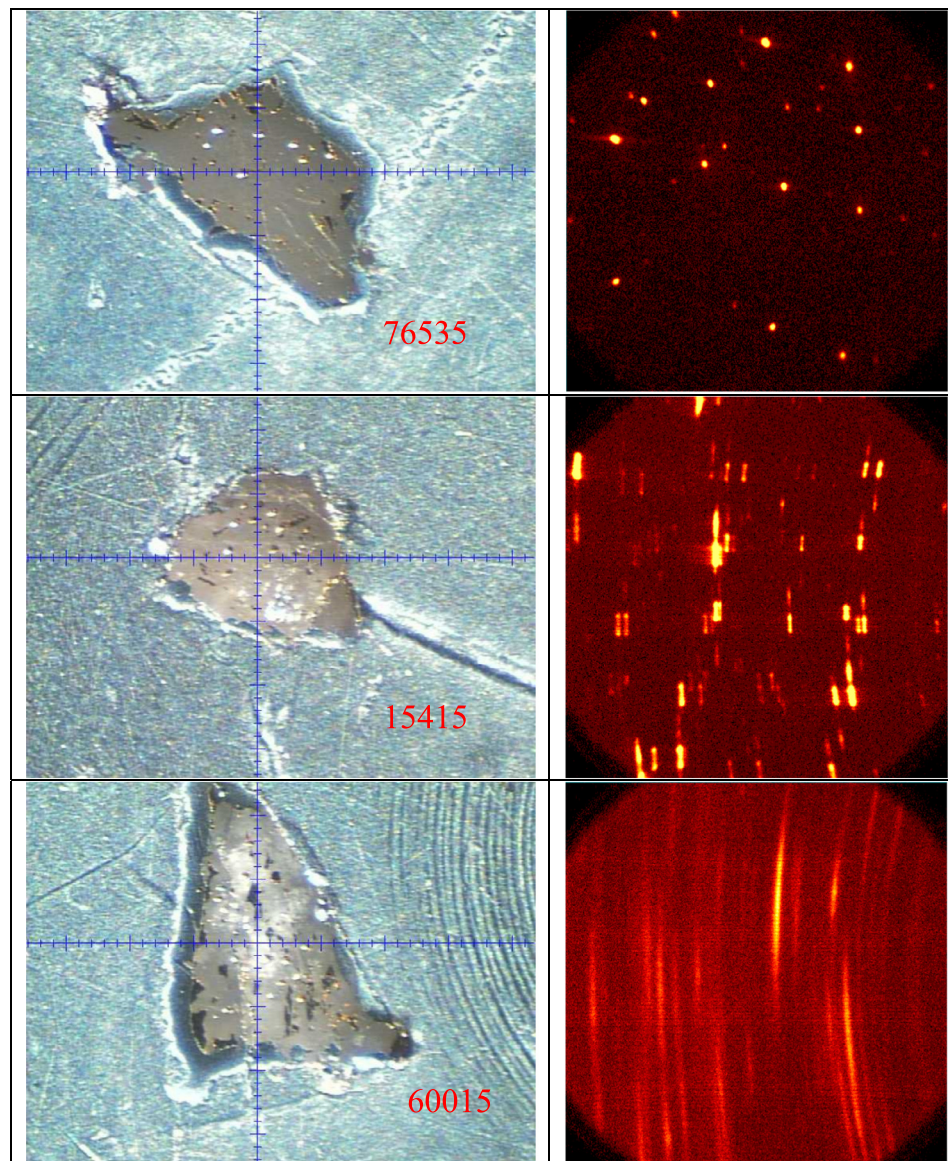
Fig. 4. Context photomicrographs of lunar plagioclase grains mounted in indium metal for prior SIMS analysis displayed next to their corresponding GADDS images (ticks are 50 μm). The X-ray diffraction patterns shown on the GADDS images go from spots (76535) to short streaks (15415) to long streaks (60015), which can be correlated to shock levels from minimal or unshocked to moderately to highly shocked respectively according to the rating scheme of Pickersgill et al. (2015).

5. Discussion

5.1. Preservation of hydrogen in lunar plagioclases during impact

The Apollo samples have often experienced varying degrees of shock-induced deformation due to intense impacts on the Moon's surface. The lunar plagioclase grains for this study also show shock features, from minimally shocked to highly shocked (Fig. 4). Our previous FTIR analyses (Hui et al., 2013), as well as the SIMS analyses in the present study, show that these lunar plagioclase grains contain water and measured water concentration (Table 1) is not related to the degree of shock. Our results are consistent with laboratory shock experiments that have demonstrated that impact does not affect water in plagioclase grains, even when highly shocked (to ∼30 GPa, Minitti et al., 2008a). Hence, it seems that the impact-induced shock effects are unlikely to account for the hydrogen compositions observed in this study. Furthermore, the results are also consistent with observations that impact may not affect water concentrations in pyroxene grains (Peslier et al., 2016).

Laboratory experiments show that the hydrous mineral amphibole could preferentially lose H over D, resulting in an increase of δD up to 87‰ during impact (Minitti et al., 2008a, 2008b). If shock indeed affects original D/H ratios of plagioclase in the same way as that in amphibole, such an increase would be within the large uncertainty of our analyses of δD in plagioclase. Therefore, it seems justified to suggest that these lunar plagioclase grains most likely preserved their magmatic δD signatures.

5.2. End members of hydrogen isotope ratio in the LMO products

It is important to know whether the water detected in ferroan anorthositic plagioclase resulted from metasomatic hydration after the FAN formation. Petrographic observations indicate FAN 60015 did not experience metasomatism by later hydrated fluids (Dixon and Papike, 1975). In fact, no evidence has been reported for any rock in the Moon that has been metasomatically hydrated. Therefore, we take the δD value of FAN 60015 to represent that of the LMO residual liquid during the crystallization of FAN 60015.
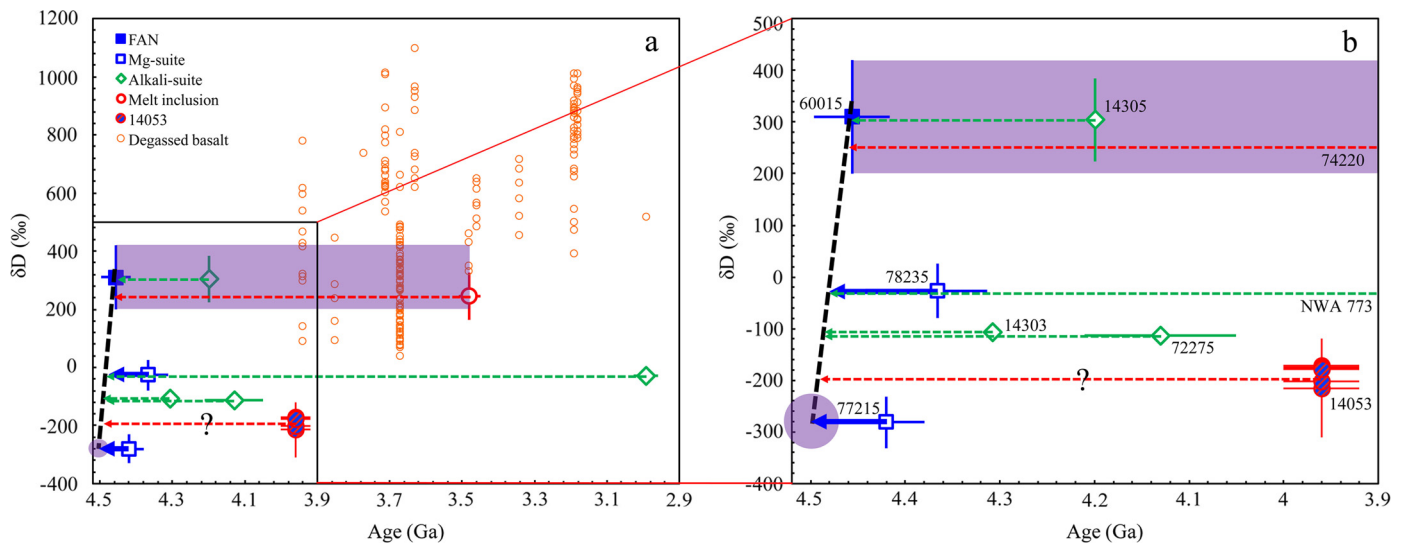
Fig. 5. Hydrogen isotope ratios (δD) versus crystallization ages of lunar plutonic rocks and basalts. All the hydrogen isotope data are from the literature (Table S1, and references therein) except the hydrogen isotope ratio of FAN 60015, which is our new datum. The δD of Mg-suite (78235, 77215), alkali-suite (14305, 14303, 72275, NWA 773) and melt inclusions (74220) are weighted average values. Ages are from the literature (Table S1, and references therein). The purple areas represent the possible δD endmembers of LMO products. The black dotted line represents the mixing trend between two end members, while the arrows point to the potential hydrogen source regions of lunar samples on the trend. Fig. 5b is a zoomed-in view of Fig. 5a at low δD and oldest ages.

The δD of FAN 60015 is within the δD range ($+187 \pm 19$ to $+327 \pm 32\permil$; Saal et al., 2013) of melt inclusions hosted in olivine of pyroclastic sample 74220 (Fig. 3). These olivine melt inclusions contain up to ~1200 ppm H_2O, similar to primitive terrestrial mid-ocean ridge basalts (Hauri et al., 2011; Chen et al., 2015). This water content has been suggested to represent relatively undegassed basaltic magma and used to calculate the water content of the mantle source region of these basalts (Hauri et al., 2011; Chen et al., 2015). The mantle source is regarded to be associated with ilmenite-rich cumulate crystallized from the LMO after the onset of formation of the lunar primary feldspathic crust (e.g., Snyder et al., 1992). Furthermore, the δD value of 60015 is indistinguishable from those ($+238 \pm 72$, $+341 \pm 53\permil$; Greenwood et al., 2011) of an apatite in a pristine cumulate alkali anorthosite 14305,303 (Fig. 3). Note that no correction of cosmic ray spallation has been applied to the δD of an apatite in 14305,303 because the contribution of spallogenic D is an order of magnitude lower than the relative high measured water content of this hydrous mineral (Greenwood et al., 2011). Sample 14305,303, however, is a plutonic sample from the highland alkali-suite and does not represent a direct product of the LMO, but may have resulted from the re-melting of evolved products related to urKREEP (primeval KREEP directly from the last dregs of LMO crystallization; Warren, 1985). Therefore, the similarity of δD in three different lithologies formed at different times suggests that the D/H ratio of the lunar interior did not change significantly after the formation of the primary lunar crust. Consequently, we suggest that our δD ($+310 \pm 110\permil$) for the late stage of LMO during the crystallization of the primary crust is consistent with this relatively constant δD of the lunar mantle through time. Although the Moon could have experienced a late heavy bombardment (Elkins-Tanton et al., 2004), the similarity of δD of FANs and of undegassed olivine melt inclusions of pyroclastic sample 74220 suggests that the formation of primary crust may have helped to prevent late addition or degassing from further affecting the δD of the LMO cumulates. The constant high δD of relatively evolved (i.e., late crystallized) products of the LMO may represent an upper limit on the primary δD during the LMO solidification.

There are primitive lunar samples with lower δD values. Lunar 74002 volcanic glasses have δD that are less heavy with a predegassing δD of $-100\permil$ (Füri et al., 2014). These volcanic glass δD

cannot be related to those of 74220 olivine-hosted melt inclusions via degassing. Furthermore, the apatites of highland norites 77215 and 78235, the only two Mg-suite samples having reliable hydrogen isotopic data, also record lower δD values, with a weighted average δD of $-281 \pm 49\permil$ and $-27 \pm 98\permil$ respectively (Barnes et al., 2014). Despite the fact that portions of norite 77215 may not be chemically pristine (Day et al., 2010), Barnes et al. (2014) argued that δD of $-281 \pm 49\permil$ represents the indigenous magmatic hydrogen isotope ratio of 77215. The apatites of granite 14303, a cumulate alkali-suite sample, also have a weighted average δD of $-105 \pm 130\permil$ (Barnes et al., 2014). The δD signature of these volcanic or plutonic samples could indicate the presence of a reservoir with negative δD residing in the lunar interior.

More information can be gathered from hydrogen isotope analyses of apatites in lunar basalts. Most of the δD values of basaltic apatites are higher than those of plutonic rocks (Fig. 5). Their relatively wide range of δD is consistent with magmatic degassing that may have fractionated H from D in these basalts or with assimilation of low δD regolith (Saal et al., 2013; Treiman et al., 2016). Therefore, the δD of these degassed basalts cannot directly reflect those of their source regions. Apatites from relatively undegassed lunar basalts, however, have been used to infer source characteristics. The δD of apatite of high-Al basalt 14053 ranges from -17 ± 100 to $-190 \pm 33\permil$ which it could have inherited from its source region (Treiman et al., 2016, and referenced therein). Alternatively, Treiman et al. (2016) have interpreted the low δD values as resulting from metasomatic addition of solar wind hydrogen. Negative δD values (Tartèse et al., 2014) have been inferred for the source region of KREEP basalt 72275 and meteorite NWA 773 from the analysis of apatites that crystallized prior to their parent-magma start of degassing.

Overall, the δD range exhibited by the plutonic rocks and "undegassed" basalt phases indicates heterogeneities of δD in the lunar mantle (Fig. 5). The δD of mantle source regions of lunar material so far fall between two end-members represented by FAN 60015 ($+310 \pm 110\permil$) and norite 77215 ($-281 \pm 49\permil$; Barnes et al., 2014) (Fig. 5). The latter is similar to the δD inferred for Earth's deep primordial mantle (Hallis et al., 2015).

Now we explore the possible relationships between the sources of the FAN and Mg-suite rocks by evaluating mixing models. It has been suggested that the samples forming the Mg-suite orig-
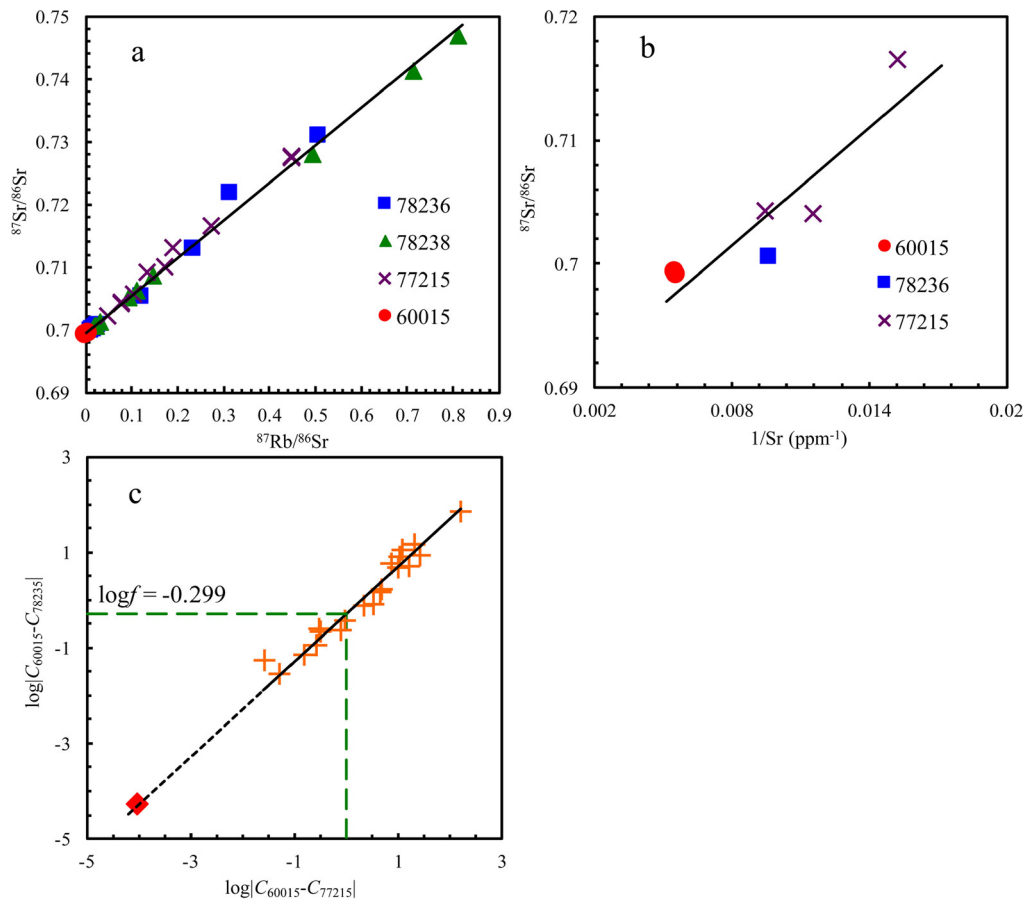
Fig. 6. Mixing trends between FAN 60015 and Mg-suite norites 77215 and 78235 (from the same boulder of 78236 and 78238). (a) Best-fit line drawn through the $^{87}Sr/^{86}Sr$ and $^{87}Rb/^{86}Sr$ ratios of mineral separates and "whole rock" of 60015, 77215, 78236, and 78238 (Table S2, and references therein). The crystallization ages of these samples are older (>4 Ga, Table S2, and references therein) than the ∼3.8 Ga calculated from this "isochron". Furthermore, FAN 60015 likely formed through a different process than the Mg-suite norites (see text for discussion) (Shearer et al., 2006 and references therein), while norite 77215 has a different isochron age than norite 78236/8 (Borg et al., 2015). The correlation of the $^{87}Sr/^{86}Sr$ and $^{87}Rb/^{86}Sr$ ratios of these lithologies can instead be interpreted as the result of mixing between FAN and a melt derived from the lunar mantle (Shearer et al., 2015) containing a unique Sr isotope signature. (b) $^{87}Sr/^{86}Sr$ ratios are positively correlated with the reciprocals of the Sr concentrations of "whole rock" of 60015, 77215, and 78236 (Table S2), confirming a mixing relationship of the sources of these three lunar samples. (c) Graphic representation of the mixing equation defined by the major- and trace-element concentrations (each orange cross represent one element; Table S3, and references therein) of FAN 60015 and Mg-suite norites 77215 and 78235. The D/H data (red diamond), which were not used in developing the mixing line, fall on the extension of this defined line. (For interpretation of the references to color in this figure legend, the reader is referred to the web version of this article.)

inated from the interaction between the hot and less dense early LMO cumulates and the base of the lunar primordial crust during cumulate pile overturn (Shearer et al., 2015). This is consistent with the Rb–Sr isotopic systematics of Mg-suite norites (77215 and 78235) and FAN 60015 that we could model with mixing equations (Figs. 6a,b). Bulk-rock major- and trace-element compositions can also be explained by source mixing between FAN 60015 and Mg-suite norites 77215 and 78235 using the equation $C_{78235} = (1 - f)C_{60015} + fC_{77215}$ (alternative format $\log|C_{60015} - C_{78235}| = \log f + \log|C_{60015} - C_{77215}|$) where f is the proportion of norite 77215 as one end-member in the mixture (Fig. 6c). The D/H ratios of these rocks, which are not used to construct this mixing equation, also fall on this mixing curve (Fig. 6c). The trace-element compositions of the alkali-suite, however, cannot be explained by simple mixing. This may be because the highland alkali-suite is more evolved than the Mg-suite even if they may be petrogenetically related (Shervais and McGee, 1998; Shearer et al., 2015). Nevertheless, the hydrogen isotope ratios of alkali-suite samples are still within the δD range bracketed by FAN 60015 and norite 77215 (Fig. 5).

It has been suggested that some anorthosites may not directly crystallize from the LMO, but were likely generated from partial melting of the lunar mantle (Gross et al., 2014). However, the

high δD value of FAN 60015 (much higher than norite) is more consistent with it being crystallized in the LMO and float to the surface to form an early primary crust (Elkins-Tanton et al., 2011). If FAN 60015 was derived from a parcel of mantle or a crustal magma reservoir associated with norites 77215 and 78235, we would expect a negative δD, similar to those of norites, because of its plutonic origin. This is not consistent with the positive value of $+310 \pm 110‰$ we observe.

In conclusion, our data coupled with those from the literature indicate there are two endmember source compositions for lunar highland rocks derived from the LMO or from partial melting of the cumulate mantle source. FAN samples and derivatives of more evolved LMO products having a positive δD, and the more mafic endmember having a negative δD. The more mafic endmember came from a deeper source and may represent derivatives from early LMO crystallization (Shearer et al., 2015), and the FAN endmember represents a source derived from a more evolved LMO. The hydrogen isotope data are consistent with the LMO producing a heterogeneous cumulate interior via degassing. The source of the FANs is the top part of the LMO, which experienced the strongest effects of degassing. This hydrogen degassing model in the LMO is consistent with other volatile elements, such as Zn, Cl, S and K (Day and Moynier, 2014; Boyce et al., 2015).

5.3. Speculation on the degassing of the LMO and initial water content

The increase of δD in the LMO cumulates could have resulted from degassing as crystallization proceeded. In this scenario, the primordial Moon at the beginning of LMO would have a δD of about $-280‰$, similar to that of the Earth (Usui et al., 2012; Hallis et al., 2015), which is consistent with conclusions based on other isotopic systems (e.g., Dauphas et al., 2014). The FAN suite formed near the end of LMO evolution, and the highly positive δD is consistent with isotope fractionation by degassing. We interpret the high δD of FAN as representing the δD signature of the late LMO cumulates and the low δD of Mg-suite norites representing the δD signature of the early LMO cumulates (Figs. 5 and 6). The change of D/H ratio during volatile loss by Rayleigh fractionation from the LMO into a vacuum can be given by $\frac{R}{R_0} = F^{\sqrt{M_1/M_2}-1}$, where R is the D/H ratio of the LMO when a fraction F of hydrogen remains in the LMO, and R_0 is the initial D/H ratio of the LMO, and M_1 and M_2 are the masses of the volatile phase isotopologues (Sharp et al., 2013). We assume that a δD of $-280‰$ represents that of the initial LMO, especially as it is comparable to the δD of some CI, CO and CM chondrites (Alexander et al., 2012), of the proto-Earth mantle (Palme and O'Neill, 2007; Barnes et al., 2014), and of the primordial water in Earth's deep mantle (Hallis et al., 2015). Approximately 96.2% degassing of molecular H_2 (masses of 2.016 for H_2, and 3.022 for HD) would be needed to raise the δD of the LMO residue to $+310‰$ at the time of the crystallization of FAN (Fig. 7). This amount of degassing of the LMO is consistent with that inferred from other volatile elements such as S, Cl, K, and Zn (Day and Moynier, 2014; Boyce et al., 2015). In contrast, degassing of H_2O (masses of 18.015 for H_2O, and 19.021 for HDO) would require the loss of $>99.99\%$ of the total water in the LMO to reach this high δD of FAN (Fig. 7), which would mean an unrealistic amount of water in the initial LMO. Moreover, degassing of H_2 has been proposed for degassing of lunar basalts due to the low oxygen fugacity of the Moon (Saal et al., 2013; Sharp et al., 2013; Barnes et al., 2014). We conclude that the hydrogen isotope ratios of the lunar mantle were controlled by H_2 degassing during the crystallization of the LMO (Fig. 7). Note that the process of LMO crystallization itself can increase water content in the residual melt. The isotopic effects of degassing on water content in the LMO melt imply that the initial LMO before degassing may contain high H_2O, and the exact concentration depends on the adopted hydrogen partition coefficient between plagioclase and melt. If a partition coefficient of 0.005 ± 0.003 (Hamada et al., 2013; combined with the latest infrared absorption coefficient determined for water in plagioclase by Mosenfelder et al., 2015) is adopted, the initial H_2O concentration in the primitive LMO would be $5000 \,^{+6600}_{-2900}$ ppm using water in the LMO residue equilibrated with FAN 60015 plagioclase (5 ± 1 ppm water; Table 1). If a new partition coefficient is used of 0.02 ± 0.002 determined under the lunar reduced conditions by Caseres et al. (2017), which is also in the range of 0.006–0.04 as determined by Lin et al. (2017), the calculated initial LMO water content would be $1320 \,^{+1240}_{-680}$ ppm. Note that if the generic partition coefficient of 0.001 used by Elkins-Tanton and Grove (2011) in their LMO model is also used here, the initial LMO water content would be as high as ~ 2.6 wt%. Therefore, an accurate hydrogen partition coefficient between plagioclase and lunar melt is needed to model the degassing process in the LMO.

The hydrogen and therefore water content in the melt residue is expected to have increased as the LMO crystallization proceeded. However, most of the volatiles in the melt residue would have been lost due to the degassing of the LMO. The giant impact may not have caused significant devolatilization of the water,
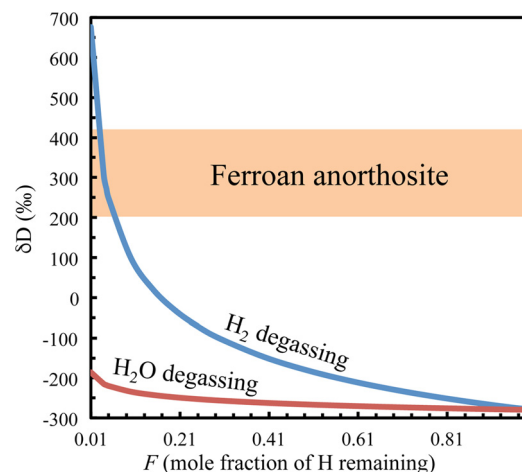

Fig. 7. Calculated δD in the melt for degassing assuming Rayleigh fractionation into a vacuum for H_2 (masses 2.016 and 3.022, fractionation factor $(2.016/3.022)^{1/2}$) and H_2O (masses 18.015 and 19.021, fractionation factor $(18.015/19.021)^{1/2}$) following the procedure of Sharp et al. (2013). The shaded area indicates the δD range of FAN 60015.

Zn (Day and Moynier, 2014; Day et al., 2017) and Cl (Boyce et al., 2015) from the Moon-forming material.

6. Summary

The available lunar hydrogen isotope data are consistent with a LMO having an initial δD of about $-280‰$, which was increased to about $+310‰$ at the time of formation of ferroan anorthositic crust by losing $\geq 96.2\%$ of the initial hydrogen content through degassing of molecular H_2 under reducing conditions. In the context of this model, the deeper and more primitive lunar interior has a negative δD of $-280‰$, whereas the more degassed shallow mantle and crust of the Moon has higher δD of $+310‰$. Mixing of the two source reservoirs would generate intermediate δD values. Alternatively, different degrees of degassing in the LMO could also have produced mantle cumulates with different δD between these two end members. Further degassing at the time of eruption of mare basaltic magma would lead to even higher δD up to $+1000‰$ in late stage apatite and pyroclastic glass. The heterogeneous hydrogen isotope ratio of the lunar interior suggests that other planets and satellites may also contain reservoirs in their interior with different hydrogen compositions, both elemental and isotopic, if the different layers have not been homogenized by mantle convection/cumulate overturn, which has also been suggested from other volatile elements (e.g., Day and Moynier, 2014; Boyce et al., 2015).

Appendix A. Supplementary material

Supplementary material related to this article can be found online at http://dx.doi.org/10.1016/j.epsl.2017.05.029.

References

Albarède, F., Albalat, E., Lee, C.-T.A., 2015. An intrinsic volatility scale relevant to the Earth and Moon and the status of water in the Moon. Meteorit. Planet. Sci. 50, 568–577.

Alexander, C.M.O'D., et al., 2012. The provenances of asteroids, and their contributions to the volatile inventories of the terrestrial planets. Science 337, 721–723.

Anand, M., Tartèse, R., Barnes, J.J., 2014. Understanding the origin and evolution of water in the Moon through lunar sample studies. Philos.Trans. R. Soc. A 372, 20130254.

Barnes, J.J., et al., 2014. The origin of water in the primitive Moon as revealed by the lunar highlands samples. Earth Planet. Sci. Lett. 390, 244–252.

Barnes, J.J., et al., 2016. An asteroidal origin for water in the Moon. Nat. Commun. 7, 11684. http://dx.doi.org/10.1038/ncomms11684.

Bell, D.R., Ihinger, P.D., 2000. The isotopic composition of hydrogen in nominally anhydrous mantle minerals. Geochim. Cosmochim. Acta 64, 2109–2118.

Borg, L.E., Connelly, J.N., Boyet, M., Carlson, R.W., 2011. Chronological evidence that the Moon is either young or did not have a global magma ocean. Nature 477, 70–72.

Borg, L.E., Gaffney, A.M., Shearer, C.K., 2015. A review of lunar chronology revealing a preponderance of 4.34–4.37 Ga ages. Meteorit. Planet. Sci. 50, 715–732.

Boyce, J.W., Tomlinson, S.M., McCubbin, F.M., Greenwood, J.P., Treiman, A.H., 2014. The lunar apatite paradox. Science 344, 400–402.

Boyce, J.W., et al., 2010. Lunar apatite with terrestrial volatile abundances. Nature 466, 466–469.

Boyce, J.W., et al., 2015. The chlorine isotope fingerprint of the lunar magma ocean. Sci. Adv. 1, e1500380.

Caseres, J.R., Mosenfelder, J.L., Hirschmann, M.M., 2017. Partitioning of hydrogen and fluorine between feldspar and melt under the conditions of lunar crust formation. In: 48th Lunar Planet. Sci. Conf. Abstract #2303.

Chen, Y., et al., 2015. Water, fluorine, and sulfur concentrations in the lunar mantle. Earth Planet. Sci. Lett. 427, 37–46.

Dauphas, N., Burkhardt, C., Warren, P.H., Teng, F.-Z., 2014. Geochemical arguments for an Earth-like Moon-forming impactor. Philos.Trans. R. Soc. A 372, 251–255.

Day, J.M.D., Moynier, F., 2014. Evaporative fractionation of volatile stable isotopes and their bearing on the origin of the Moon. Philos.Trans. R. Soc. A 372, 20130259.

Day, J.M.D., Moynier, F., Meshik, A.P., Pradivtseva, O.V., Petit, D.R., 2017. Evaporative fractionation of zinc during the first nuclear detonation. Sci. Adv. 3, e1602668.

Day, J.M.D., Walker, R.J., James, O.B., Puchtel, I.S., 2010. Osmium isotope and highly siderophile element systematics of the lunar crust. Earth Planet. Sci. Lett. 289, 595–605.

Dixon, J.R., Papike, J.J., 1975. Petrology of anorthosites from the Descartes region of the moon: Apollo 16. Proc. Lunar Sci. Conf. 6, 263–291.

Dymek, R.F., Albee, A.L., Chodos, A.A., 1975. Comparative petrology of lunar cumulate rocks of possible primary origin: dunite 72415, troctolite 76535, norite 78235, and anorthosite 62237. Proc. Lunar Sci. Conf. 6, 301–341.

Elkins-Tanton, L.T., Hager, B.H., Grove, T.L., 2004. Magmatic effects of the lunar late heavy bombardment. Earth Planet. Sci. Lett. 222, 17–27.

Elkins-Tanton, L.T., Grove, T.L., 2011. Water (hydrogen) in the lunar mantle: results from petrology and magma ocean modeling. Earth Planet. Sci. Lett. 307, 173–179.

Elkins-Tanton, L.T., Burgess, S., Yin, Q.-Z., 2011. The lunar magma ocean: reconciling the solidification process with lunar petrology and geochronology. Earth Planet. Sci. Lett. 304, 326–336.

Eugster, O., et al., 1984. Cosmic ray exposure histories of Apollo 14, Apollo 15, and Apollo 16 rocks. In: Proc. Lunar Planet. Sci. Conf., vol. 14, pp. B498–B512.

Flemming, R.L., 2007. Micro X-ray Diffraction (μXRD): a versatile technique for characterization of Earth and planetary materials. Can. J. Earth Sci. 44, 1333–1346.

Füri, E., Deloule, E., Gurenko, A., Marty, B., 2014. New evidence for chondritic lunar water from combined D/H and noble gas analyses of single Apollo 17 volcanic glasses. Icarus 229, 109–120.

Greenwood, J.P., et al., 2011. Hydrogen isotope ratios in lunar rocks indicate delivery of cometary water to the Moon. Nat. Geosci. 4, 79–82.

Gross, J., Treiman, A.H., Mercer, C.N., 2014. Lunar feldspathic meteorites: constraints on the geology of the lunar highlands, and the origin of the lunar crust. Earth Planet. Sci. Lett. 388, 318–328.

Hallis, L.J., et al., 2015. Evidence for primordial water in Earth's deep mantle. Science 350, 795–797.

Hamada, M., Ushioda, M., Fujii, T., Takahashi, E., 2013. Hydrogen concentration in plagioclase as a hygrometer of arc basaltic melts: approaches from melt inclusion analyses and hydrous melting experiments. Earth Planet. Sci. Lett. 365, 253–262.

Hauri, E., et al., 2002. SIMS analysis of volatiles in silicate glasses 1. Calibration, matrix effects and comparison with FTIR. Chem. Geol. 183, 99–114.

Hauri, E.H., Weinreich, T., Saal, A.E., Rutherford, M.C., Van Orman, J.A., 2011. High-pre-eruptive water contents preserved in lunar melt inclusions. Science 333, 213–215.

Hörz, F., Gibbons, R.V., Gault, D.E., Hartung, J.B., Brownlee, D.E., 1975. Some correlation of rock exposure ages and regolith dynamics. Proc. Lunar Sci. Conf. 6, 3495–3508.

Hui, H., Peslier, A.H., Zhang, Y., Neal, C.R., 2013. Water in lunar anorthosites and evidence for a wet early Moon. Nat. Geosci. 6, 177–180.

Kato, C., Moynier, F., Valdes, M.C., Dhaliwal, J.K., Day, J.M.D., 2015. Extensive volatile loss during formation and differentiation of the Moon. Nat. Commun. 6, 7617. http://dx.doi.org/10.1038/ncomms8617.

Lin, Y., et al., 2017. A lunar hygrometer based on plagioclase-melt partitioning of hydrogen. In: 48th Lunar Planet. Sci. Conf. Abstract #1286.

Liu, Y., et al., 2012. Direct measurement of hydroxyl in the lunar regolith and the origin of lunar surface water. Nat. Geosci. 5, 779–782.

Lugmair, G.W., Marti, K., Kurtz, J.P., Scheinin, N.B., 1976. History and genesis of lunar troctolite 76535 or: how old is old?, Proc. Lunar Sci. Conf. 7, 2009–2033.

McCubbin, F.M., et al., 2010. Nominally hydrous magmatism on the Moon. Proc. Natl. Acad. Sci. USA 107, 11223–11228.

McGee, J.J., 1993. Lunar ferroan anorthosites: mineralogy, compositional variations, and petrogenesis. J. Geophys. Res. 98, 9089–9105.

Mills, R.D., Simon, J.I., Alexander, C.M.O'D., Wang, J., Hauri, E.H., 2017. Water in alkali feldspar: the effect of rhyolite generation on the lunar hydrogen budget. Geochem. Persp. Let. 3, 115–123.

Minitti, M.E., Rutherford, M.J., Taylor, B.E., Dyar, M.D., Schultz, P.H., 2008a. Assessment of shock effects on amphibole water contents and hydrogen isotope compositions: A. Amphibole experiments. Earth Planet. Sci. Lett. 266, 46–60.

Minitti, M.E., et al., 2008b. Assessment of shock effect on amphibole water contents and hydrogen isotope compositions: 2. Kaersutitic amphibole experiments. Earth Planet. Sci. Lett. 266, 288–302.

Morgan, J.W., Krähenbühl, U., Ganapathy, R., Anders, E., 1972. Trace elements in Apollo 15 samples: implications for meteorite influx and volatile depletion on the Moon. Geochim. Cosmochim. Acta, Suppl. 3, 1361–1376.

Mosenfelder, J.L., et al., 2011. Analysis of hydrogen in olivine by SIMS: evaluation of standards and protocol. Am. Mineral. 96, 1725–1741.

Mosenfelder, J.L., Rossman, G.R., Johnson, E.A., 2015. Hydrous species in feldspars: a reassessment based on FTIR and SIMS. Am. Mineral. 100, 1209–1221.

Norman, M.D., Borg, L.E., Nyquist, L.E., Bogard, D.D., 2003. Chronology, geochemistry, and petrology of a ferroan noritic anorthosite clast from Descartes breccia 67215: clues to the age, origin, structure, and impact history of the lunar crust. Meteorit. Planet. Sci. 38, 645–661.

Palme, H., O'Neill, H.St.C., 2007. Cosmochemical estimates of mantle composition. Treat. Geochem. 2, 1–38.

Paniello, R.C., Day, J.M.D., Moynier, F., 2012. Zinc isotopic evidence for the origin of the Moon. Nature 490, 376–379.

Peslier, A.H., Cintala, M.J., Cardenas, F., Montes, R., 2016. Effect of Shock on H in Martian Meteorite Pyroxene via Analogue Impact Experiments. Goldschmidt conference, Yokohama, June 26–July 1.

Pickersgill, A.E., Flemming, R.L., Osinski, G.R., 2015. Toward quantification of strain-related mosaicity in shocked lunar and terrestrial plagioclase by in situ micro-X-ray diffraction. Meteorit. Planet. Sci. 50, 1851–1862.

Robinson, K.L., Taylor, G.J., 2014. Heterogeneous distribution of water in the Moon. Nat. Geosci. 7, 401–408.

Robinson, K.L., et al., 2016. Water in evolved lunar rocks: evidence for multiple reservoirs. Geochim. Cosmochim. Acta 188, 244–260.

Saal, A.E., et al., 2008. Volatile content of lunar volcanic glasses and the presence of water in the Moon's interior. Nature 454, 192–195.

Saal, A.E., Hauri, E.H., Van Orman, J.A., Rutherford, M.J., 2013. Hydrogen isotopes in lunar volcanic glasses and melt inclusions reveal a carbonaceous chondrite heritage. Science 340, 1317–1320.

Sharp, Z.D., McCubbin, F.M., Shearer, C.K., 2013. A hydrogen-based oxidation mechanism relevant to planetary formation. Earth Planet. Sci. Lett. 380, 88–97.

Sharp, Z.D., Shearer, C.K., McKeegan, K.D., Barnes, J.D., Wang, Y.Q., 2010. The chlorine isotope composition of the moon and implications for an anhydrous mantle. Science 329, 1050–1053.

Shearer, C.K., Elardo, S.M., Petro, N.E., Borg, L.E., McCubbin, F.M., 2015. Origin of the lunar highlands Mg-suite: an integrated petrology, geochemistry, chronology, and remote sensing perspective. Am. Mineral. 100, 294–325.

Shearer, C.K., et al., 2006. Thermal and magmatic evolution of the Moon. Rev. Mineral. Geochem. 60, 365–518.

Shervais, J.W., McGee, J.J., 1998. Ion and electron microprobe study of troctolites, norite, and anorthosites from Apollo 14: evidence for urKREEP assimilation during petrogenesis of Apollo 14 Mg-suite rocks. Geochim. Cosmochim. Acta 62, 3009–3023.

Snyder, G.A., Taylor, L.A., Neal, C.R., 1992. A chemical model for generating the sources of mare basalt: combined equilibrium and fractional crystallization of the lunar magmasphere. Geochim. Cosmochim. Acta 56, 3809–3823.

Stephant, A., Robert, F., 2014. The negligible chondritic contribution in the lunar soils water. Proc. Natl. Acad. Sci. USA 111, 15007–15012.

Tartèse, R., et al., 2013. The abundance, distribution, and isotopic composition of hydrogen in the Moon as revealed by basaltic lunar samples: implications for the volatile inventory of the Moon. Geochim. Cosmochim. Acta 122, 58–74.

Tartèse, R., et al., 2014. Apatites in lunar KREEP basalts: the missing link to understanding the H isotope systematics of the Moon. Geology 42, 363–366.

Taylor, S.R., Pieters, C.M., MacPherson, G.J., 2006. Earth–Moon system, planetary science, and lessons learned. Rev. Mineral. Geochem. 60, 657–704.

Treiman, A.H., et al., 2016. D-poor hydrogen in lunar mare basalts assimilated from lunar regolith. Am. Mineral. 101, 1596–1603.

Usui, T., Alexander, C.M.O'D., Wang, J., Simon, J.I., Jones, J.H., 2012. Origin of water and mantle–crust interactions on Mars inferred from hydrogen isotopes and volatile element abundances of olivine-hosted melt inclusions of primitive shergottites. Earth Planet. Sci. Lett. 357–358, 119–129.

Wang, K., Jacobsen, S.B., 2016. Potassium isotopic evidence for a high-energy giant impact origin of the Moon. Nature 538, 487–490.

Warren, P.H., 1985. The magma ocean concept and lunar evolution. Annu. Rev. Earth Planet. Sci. 13, 201–240.

Waythomas, C.F., et al., 2010. The 7–8 August 2008 eruption of Kasatochi Volcano, central Aleutian Islands, Alaska. J. Geophys. Res. 115, B00B06. http://dx.doi.org/10.1029/2010JB007437.

Supplementary Information

Negligible effects from sample preparation

No OH bands have been observed in the dehydrated grains of An_{68-70}, An_{96}, and GRR 2058 using FTIR. Furthermore, the unheated An_{68-70} and An_{96} grains contain 10 and 7 ppm H_2O, respectively (Table 1), while the dehydrated grains of An_{68-70}, An_{96}, and GRR 2058 all display uniform $OH^-/^{30}Si^-$ values, lower than that of the unheated GRR 2058 (~1 ppm) (Fig. 2). Therefore, these dehydrated grains have lost their original OH contents, any hydrogen detected in the dehydrated grains is assumed to be background in the SIMS measurements, and sample preparation has not introduced additional hydrogen signal.

Hydrogen isotope fractionation between mineral and melt

No experimental studies have been carried out on the fractionation of hydrogen isotope between mineral and melt. The fractionation during mantle melting and magma differentiation, however, have been discussed using hydrogen isotope ratios of fresh submarine basalts (Kyser and O'Neil, 1984; Bindeman et al., 2012). It has been suggested differentiation or partial melting have had little effect on the hydrogen isotope fractionation (Kyser and O'Neil, 1984; Bindeman et al., 2012). Melt-lherzolite fractionation of hydrogen isotope has been suggested to be less than 10‰ during mantle melting (Bindeman et al., 2012). The uncertainties of δD of undegassed lunar minerals are rather large, typically >100‰ (Barnes et al., 2014). Therefore, the δD of lunar plutonic minerals could represent those of their parent magmas.

The δD value of GRR1968

The low water content (70 ppm) of GRR 1968 has made the determination of its hydrogen isotope ratio using traditional method (e.g., mass spectrometer) on bulk sample difficult. In this study, we use an alternative approach to calculate the δD value of GRR1968.

GRR1968 is an anorthite ($An_{93.8}Ab_{4.0}$ with 0.37% of FeO) megacryst of island arc basalt from Miyake Island of Izu-Bonin-Mariana island arc (Kimata et al., 1995; Johnson and Rossman, 2003). Because the fractionation of hydrogen isotope between mineral and melt is very small (see text above), we could use the melt δD value to represent that of GRR1968. No hydrogen isotope ratios have been published for arc basalts from Miyake Island. Therefore, we use the average δD value (-42 ± 29‰) of samples from Izu-Bonin-Mariana arc system found in the literature. This dataset includes 87 samples with δD varying from -12 to -73.7‰ (Table S4, and references therein). Furthermore, it has been suggested that the fractionation of hydrogen isotope between mineral and melt is less than 10‰ (Kyser and O'Neil, 1984; Bindeman et al., 2012). Therefore, we estimate that the δD value of GRR1968 is -42 ± 39‰. This δD estimation is reasonable and sufficiently precise for the purpose of our study, because most of the uncertainties in the H isotopic results of lunar plagioclases are from the correction for cosmogenic production of hydrogen. Furthermore, the δD of An_{96}, a plagioclase from Aleutian arc melt (Waythomas et al., 2010), is -10 ± 90‰ using this standard GRR1968 (-42 ± 39‰), overlapping with those (-12 to -73.7‰) from Izu-Bonin-Mariana arc system (Table S4, and references therein).

Estimation of the initial LMO water content

The plagioclase of ferroan anorthosite 60015 contains 5 ± 1 ppm water analyzed by SIMS. Using a plagioclase-melt partition coefficient (Hamada et al., 2013; 0.005 ± 0.003 if the

latest infrared absorption coefficient determined for water in plagioclase by Mosenfelder et al. (2015) is used), the LMO melt that equilibrated with the ferroan anorthositic plagioclase could have contained 1000 ppm water. The relatively large uncertainty primarily comes from that of partition coefficient. Water in the LMO could be lost through degassing into a vacuum. On the other hand, water in the LMO melt could increase as the LMO solidification continued. If only these two scenarios were considered, we can infer the initial LMO water content.

The hydrogen species degassed in the Moon has been suggested to be H_2 (Sharp et al., 2013). The fraction of hydrogen (equivalent to water) lost from the LMO into a vacuum before the crystallization of ferroan anorthosite can be estimated using the Rayleigh fractionation equation $\frac{R}{R_0} = F^{\sqrt{M_1/M_2}-1}$, where R is the D/H ratio of the LMO when a fraction F of hydrogen remains in the LMO, and R_0 is the initial hydrogen isotope ratio of the LMO, and M_1 and M_2 are the masses of the volatile phase isotopologues (masses of 2.016 for H_2, and 3.022 for HD; Sharp et al., 2013). The δD of -281 ± 49‰ (represented by sample 77215) is used as the initial hydrogen isotope ratio of the LMO, whereas +310 ± 110‰ (represented by sample 60015) is used as the final hydrogen isotope ratio of the LMO. Therefore, the fraction of hydrogen remained in the LMO when 60015 crystallized is 3.8%. Furthermore, 20 ± 5% of the LMO may have remained melt when ferroan anorthositic plagioclase crystallized (Shearer et al., 2006; Elkins-Tanton et al., 2011). Note almost all of the water undegassed from the LMO (i.e., 3.8% of initial LMO water) should have still remained in the LMO melt residue. Therefore, the initial LMO water content could have been up to 5000 $\pm^{6600}_{2900}$ ppm. If a new partition coefficient of 0.02 ± 0.002 determined under the lunar condition by Caseres et al. (2017), which is also in the range of 0.006 − 0.04 determined by Lin et al. (2017), is used, the calculated initial LMO water content would be 1320 $\pm^{1240}_{680}$ ppm. However, if a generic partition coefficient of 0.001 used by Elkins-Tanton and Grove (2011) in their LMO model is also used here, the initial LMO water content would be ~2.6 wt%. Therefore, an accurate hydrogen partition coefficient between plagioclase and lunar melt is needed to model the degassing process in the LMO.

References:
Barnes, J.J., et al., 2014. The origin of water in the primitive Moon as revealed by the lunar highlands samples. Earth Planet. Sci. Lett. 390, 244-252.
Bindeman, I.N., Kamenetsky, V.S., Palandri, J., Vennemann, T., 2012. Hydrogen and oxygen isotope behaviors during variable degrees of upper mantle melting: Example from the basaltic glasses from Macquarie Island. Chem. Geol. 310-311, 126-136.
Caseres, J. R., Mosenfelder, J. L., Hirschmann, M. M., 2017. Partitioning of hydrogen and fluorine between feldspar and melt under the conditions of lunar crust formation. 48th Lunar Planet. Sci. Conf., Abstract #2303.
Elkins-Tanton, L.T., Burgess, S., Yin, Q.-Z., 2011. The lunar magma ocean: Reconciling the solidification process with lunar petrology and geochronology. Earth Planet. Sci. Lett. 304, 326-336.
Elkins-Tanton, L.T., Grove, T.L., 2011. Water (hydrogen) in the lunar mantle: Results from petrology and magma ocean modeling. Earth Planet. Sci. Lett. 307, 173-179.
Hamada, M., Ushioda, M., Fujii, T., Takahashi, E., 2013. Hydrogen concentration in plagioclase as a hygrometer of arc basaltic melts: Approaches from melt inclusion analyses and hydrous melting experiments. Earth Planet. Sci. Lett. 365, 253-262.

Johnson, E.A., Rossman, G.R., 2003. The concentration and speciation of hydrogen in feldspars using FTIR and ^{1}H MAS NMR spectroscopy. Am. Mineral. 88, 901-911.

Kimata, M., et al., 1995. Anorthite megacrysts from island arc basalts. Mineral. Mag. 59, 1-14.

Kyser, T.K., O'Neil, J.R., 1984. Hydrogen isotope systematics of submarine basalts. Geochim. Cosmochim. Acta 48, 2123-2133.

Lin, Y., et al., 2017. A lunar hygrometer based on plagioclase-melt partitioning of hydrogen. 48th Lunar Planet. Sci. Conf., Abstract #1286.

Sharp, Z.D., McCubbin, F.M., Shearer, C.K., 2013. A hydrogen-based oxidation mechanism relevant to planetary formation. Earth Planet. Sci. Lett. 380, 88-97.

Shearer, C.K., et al., 2006. Thermal and magmatic evolution of the Moon. Rev. Mineral. Geochem. 60, 365-518.

Waythomas, C.F., et al., 2010. The 7-8 August 2008 eruption of Kasatochi Volcano, central Aleutian Islands, Alaska. J. Geophys. Res. 115, B00B06, doi:10.1029/2010JB007437.